Discovery and optimization of a novel, selective and brain penetrant M$_1$ positive allosteric modulator (PAM): The development of ML169, an MLPCN probe

Paul R. Reid [e,†], Thomas M. Bridges [a,d,†], Douglas J. Sheffler [a,c], Hyekyung P. Cho [a,d], L. Michelle Lewis [e], Emily Days [e], J. Scott Daniels [a,c,d], Carrie K. Jones [a,c,d,f], Colleen M. Niswender [a,c,d], C. David Weaver [a,d,e], P. Jeffrey Conn [a,c,d], Craig W. Lindsley [a,b,c,d,e], Michael R. Wood [a,c,d,*]

[a] Department of Pharmacology, Vanderbilt University Medical Center, Nashville, TN 37232, USA
[b] Department of Chemistry, Vanderbilt University, Nashville, TN 37232, USA
[c] Vanderbilt Program in Drug Discovery, Nashville, TN 37232, USA
[d] Vanderbilt Specialized Chemistry Center(MLPCN), Nashville, TN 37232, USA
[e] Vanderbilt Institute of Chemical Biology/Chemical Synthesis Core, Nashville, TN 37232, USA
[f] U.S. Department of Veterans Affairs, Tennessee Valley Healthcare System, Nashville, TN 37212, USA

ARTICLE INFO

ABSTRACT

This Letter describes a chemical lead optimization campaign directed at VU0108370, a weak M$_1$ PAM hit with a novel chemical scaffold from a functional HTS screen within the MLPCN. An iterative parallel synthesis approach rapidly established SAR for this series and afforded VU0405652 (ML169), a potent, selective and brain penetrant M$_1$ PAM with an in vitro profile comparable to the prototypical M$_1$ PAM, BQCA, but with an improved brain to plasma ratio.

© 2010 Elsevier Ltd. All rights reserved.

The muscarinic acetylcholine receptors (mAChRs) are members of the family A G-protein-coupled receptors (GPCRs) and include five subtypes denoted M$_1$–M$_5$. All five of the mAChRs are known to play critical roles in multiple basic physiological processes and represent attractive therapeutic targets for a number of peripheral and CNS pathologies.[1–3] Within the mAChRs, a major challenge has been a lack of subtype selective ligands to study the specific contribution of discrete mAChRs in various disease states.[3,4] To address this limitation, we have focused on targeting allosteric sites on mAChRs as a means to develop subtype selective small molecules, both allosteric agonists and positive allosteric modulators (PAMs).[5–9] Moreover, the emerging phenomenon of ligand-biased signaling requires the development of diverse chemical scaffolds of M$_1$ ligands to successfully dissect of the roles of M$_1$ activation through multiple, discrete ligand-biased signaling pathways.[10,11]

As members of the Molecular Libraries Production Center Network (MLPCN),[12] we performed a real-time cell-based calcium-mobilization assay employing a rat M$_1$/CHO cell line (Z' averaged 0.7) and screened a 63,656 member MLPCN compound library following a triple-add protocol to simultaneously identify M$_1$ antagonists, agonists (both orthosteric and allosteric) and positive allosteric modulators (PAMs). This screen proved to be a major success providing viable leads that were optimized into potent and highly selective M$_1$ ligands (Fig. 1): an M$_1$ antagonist (**1**, VU0255035, ML012),[13] an M$_1$ allosteric agonist (**2**, VU0357017, ML071),[14] and both an M$_1$ PAM (**3**, VU0366369, ML137)[15] and the first M$_5$ PAM (**4**, VU0238429, ML129)[16] derived from a pan-M$_1$,M$_3$,M$_5$-PAM (**5**, VU0119498).[17,18] However, the brain penetration (brain$_{AUC}$/plasma$_{AUC}$ = 0.1) and efficacy (60% ACh Max) of **3** were poor, as was the brain penetration of the prototypical M$_1$ PAM, BQCA (**6**, brain$_{AUC}$/plasma$_{AUC}$ = 0.1)[19–21]; therefore, M$_1$ PAM ligands with improved physicochemical properties for in vivo studies and novel scaffolds to address ligand-biased signaling are required. In this Letter, we describe the development of VU0405652
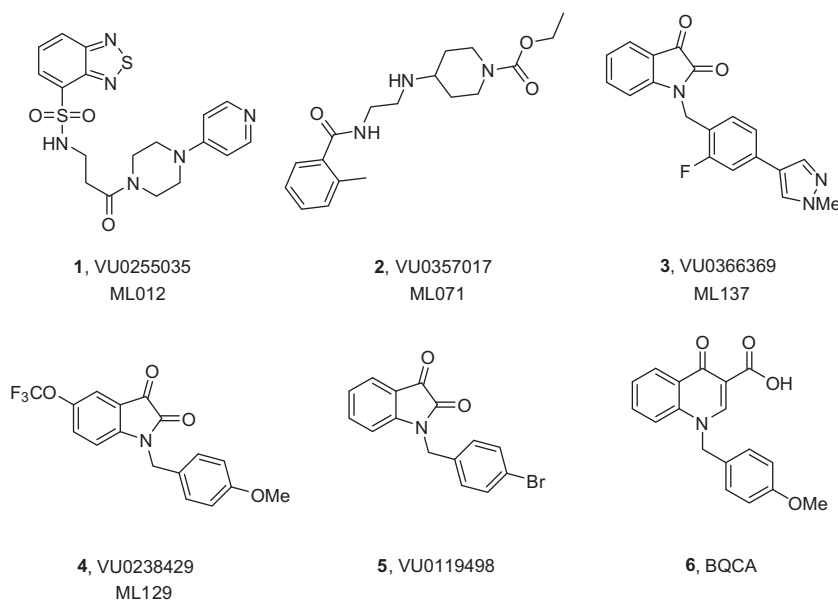
Figure 1. Structures of selective M_1 and M_5 MLPCN probes developed from hits from a triple-add functional M_1 HTS MLPCN screen (**1–5**) and BQCA (**6**).

(ML169),[22] a highly selective M_1 PAM MLPCN probe, with a novel chemical scaffold and improved brain penetration.

Perusal of the HTS data, which also yielded the non-selective hit **5**, identified a second weak M_1 PAM hit **7**, VU0108370, with an EC_{50} of ~13 μM. Confirmation of **7** from fresh powder and counter-screening against M_2–M_5 increased our enthusiasm for this highly M_1 mAChR selective hit (Fig. 2); however, the CRC did not plateau, suggesting the M_1 EC_{50} was actually >13 μM. Despite the weak potency, the confirmation of a novel M_1 PAM scaffold with high M_1 selectivity initiated a lead optimization campaign to improve M_1 potency while maintaining the high M_2–M_5 selectivity.

Our initial optimization strategy is outlined in Figure 3, and as SAR with allosteric ligands is often shallow, we employed an iterative parallel synthesis approach, along with targeted syntheses for structures encompassing more speculative modifications. Attempted modifications of the Eastern oxazole-amide, although not extensive, met with no success, returning only compounds with undetectable activity. In a straightforward attempt to reduce molecular weight the benzyl group attached to the indole nitrogen was omitted, but met with a similar lack of success (EC_{50} >10 μM) as did the sulfide and sulfoxide congeners.

Thus, we planned to hold the northern portion of **7** constant, and survey diversity on the southern benzyl moiety employing a
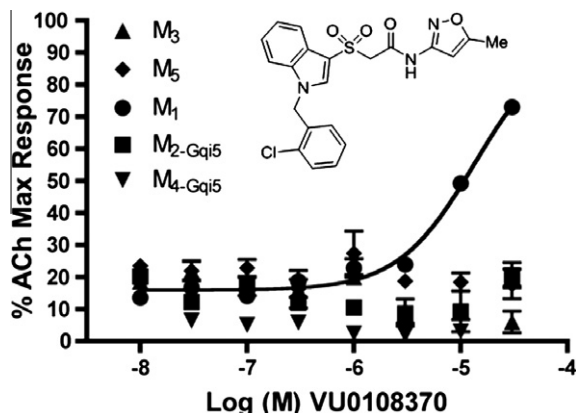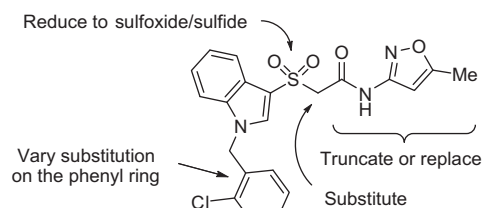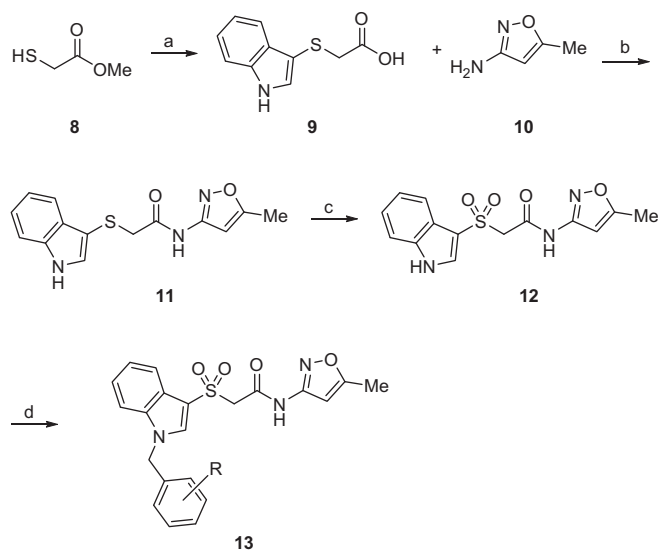

Figure 3. Initial optimization strategy for VU0108370, **7**.

Scheme 1. Reagents and conditions: (a) (i) indole, I_2, KI, MeOH, H_2O; (ii) 2 M LiOH, THF (38%); (b) PyClu, DCE, 110 °C, 20 min, mw (71%); (c) Oxone, MeOH, H_2O (88%); NaH, DMF, BnX (50–90%).

library synthesis approach. As shown in Scheme 1, the key library scaffold **12** was readily prepared in three steps from methyl thioglycolate **8**. A PyClu-mediated microwave-assisted coupling between **9** and **10** provided **11** in 71% yield, which was then oxidized to the corresponding sulfone **12** with Oxone in 88% yield.

Figure 2. Concentration response curves (CRCs) for M_1–M_5 for HTS hit VU0108370. M_1 EC_{50} ~13 μM (does not plateau) and M_2–M_5 EC_{50} >30 μM.

Table 1
Structures and activities of analogs **13**
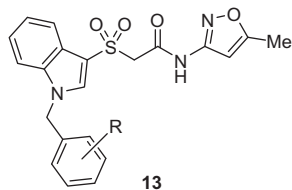
Compound	R	$M_1 EC_{50}$ (μM)[a]	%Ach Max[a]
7	2-Cl	9.71	83
13a	3-Cl	5.82	96
13b	4-Cl	>10	—
13c	2-OMe	>10	—
13d	3-OMe	6.54	79
13e	4-OMe	>10	—
13f	3-F	5.22	96
13g	3-Br	3.79	91
13h	3-CF$_3$	>10	—
13i	3-CN	>10	—
13j	3,5-diBr	>10	—
13k	3,4-diCl	>10	—
13l	4-CF$_3$	>10	—
13m	4-OCF$_3$	>10	—
13n	2-F	>10	—
13o	2,4-diF	>10	—
13p	2-Br-4-F	>10	—

[a] Average of at least three independent determinations.

An 18-membered library of analogs **13** was then prepared by treatment with NaH and 18 diverse benzyl halides.

As shown in Table 1, SAR, as with many allosteric ligands, was shallow affording only five active compounds from the eighteen synthesized. Upon resynthesis, HTS hit **7** (a 2-Cl congener) showed an EC$_{50}$ of 9.7 μM with 83% ACh Max; however, the CRC once again did not plateau. The other four actives, all with substituents in the 3-position, did afford sigmoidal CRCs with up to 96% ACh Max and EC$_{50}$s in the 3.8–6.5 μM range. The most potent analog was **13g**, a 3-Br derivative (EC$_{50}$ = 3.8 μM, 91% ACh Max) which provided a significant increase in potency, but at the cost of physiochemical properties (c Log P >4 and poor solubility). Replacement of the benzyl moiety with a pyridyl analog also led to an inactive compound (data not shown). However, this first generation library indicated that substitution at the 3-position of the benzyl moiety was preferred. This result then prompted us to employ **13g** as a starting material for a small Suzuki coupling library (Scheme 2) to replace the lipophilic bromide with various aryl and heteroaryl moieties to introduce basicity and/or polarity.

As shown in Table 2, SAR was again shallow, but we identified pyrazole as a preferred heterocyclic replacement for the bromide. *N*-Me pyrazole **14a** possessed an M$_1$ EC$_{50}$ of 3.2 μM (102% ACh Max), while the unsubstituted pyrazole congener **14b** was essentially equipotent (M$_1$ EC$_{50}$ = 2.2 μM, 90% ACh Max). Moreover, both pyrazole congeners lowered c Log P a full order of magnitude rela-

Table 2
Structures and activities of analogs **14**
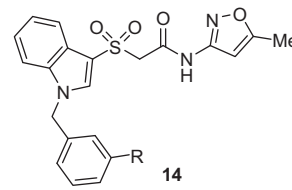
Compound	Ar/Het	$M_1 EC_{50}$ (μM)[a]	%Ach Max[a]
14a	(1-Me-pyrazol-4-yl)	3.21	102
14b	(1H-pyrazol-4-yl)	2.19	90
14c	(1-s-Bu-pyrazol-4-yl)	>10	—
14d	(phenyl)	>10	—
14e	(2-Cl-pyridin-5-yl)	>10	—
14f	(2-morpholino-pyridin-5-yl)	>10	—
14g	(2-piperazinyl-pyridin-5-yl)	>10	—
14h	(2-pyrrolidinyl-pyridin-5-yl)	>10	—

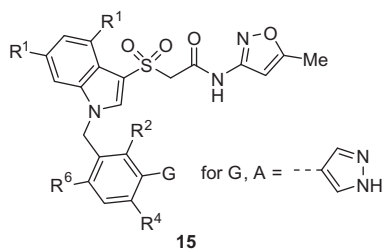[a] Average of at least three independent determinations.

tive (c Log P = 3.1) to **13g**. Additional steric bulk on the pyrazole, as in the *sec*-butyl derivative **14c**, led to an inactive analog. Phenyl derivative **14d** and basic amino pyridine analogs **14e–14h**, were inactive (M$_1$ EC$_{50}$s >10 μM).

To further the development of this novel series of M$_1$ PAMs we focused on three of the more potent analogs (**13a**, **13g** and **14b**) and applied a fine-tuning process of introducing fluorine atoms at various locations to provide analogs **15** (Table 3), an approach we found successful for multiple allosteric ligands. Across the series, substitution at the 4-position was uniformly not tolerated (**15a–c**), consistent with the SAR appearing in Table 1. Bis-fluorination of the indole ring eroded activity in the context of the bromine analog **15d** but conversely augmented the activity of the pyrazole congener **15e**. This type of subtle/confounding SAR was similarly observed with respect to fluorination at the R^2 position in analogs **15f–h**. While the presence of a fluorine at R^2 was neutral or slightly beneficial in the context of the chlorine analog (**15f**), its presence resulted in clearly decreased activity for both the bromine and pyrazole analogs, **15g** and **15h**. Lastly, the introduction of a single fluorine at the R^6 position could either be moderately detrimental in the context of pyrazole **15i** or decidedly beneficial with respect to bromine analog **15j**, where an almost 3-fold improvement in potency was observed. In this manner, both VU0405652 (**15j**) and the related difluorindole analog VU0405645 (**15e**) were chosen for further evaluation.

Both **15e** and **15j** were selective (Fig. 4A) for M$_1$ (>30 μM vs. M$_2$–M$_5$) and both compounds demonstrated impressive left-ward shifts of the ACh CRC (98-fold and 49-fold, respectively) in fold-shift assays at 30 μM (Fig. 4B), values comparable to BQCA. However, a combination of calculated properties (TPSA, Hacc, etc...), ancillary pharmacology and in vivo PK suggested **15j** was the more optimal MLPCN probe molecule compared to **15e**.

Scheme 2. Reagents and conditions: (a) Ar-B(OH)$_2$ or Het-B(OH)$_2$, 10 mol % Pd(*t*-Bu)$_2$, 1.0 M aq Cs$_2$CO$_3$, THF, mw, 120 °C (65–90%).

Table 3
Structures and activities of analogs **15**

Compound	G	R^1	R^2	R^4	R^6	$M_1EC_{50}^a$ (μM)	%Ach Max[a]
15a	A	H	H	F	H	>10	—
15b	Br	H	H	F	H	>10	—
15c	Cl	H	H	F	H	>10	—
15d	Br	F	H	H	H	5.37	103
15e	A	F	H	H	H	1.85	102
15f	Cl	H	F	H	H	5.10	56
15g	Br	H	F	H	H	>10	—
15h	A	H	F	H	H	4.40	103
15i	A	H	H	F	H	3.07	96
15j	Br	H	H	F	H	1.38	84

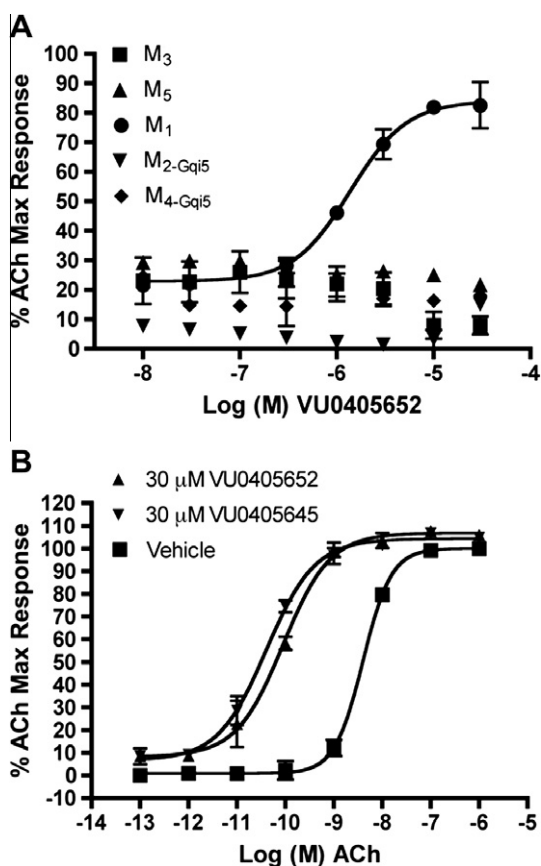[a] Average of at least three independent determinations.

Figure 4. (A) CRC for **15j**, VU0405652 at M_1–M_5 (**15e**, VU0405645 looked similar); (B) ACh fold-shift experiment at 30 μM for VU040652 (49-fold) and VU0405645 (98-fold).

In terms of ancillary pharmacology, the Lead Profile screen at Ricerca, evaluating 68 GPCRs, ion channels and transporters in radioligand binding assays, resulted in only two significant activities (DAT, 83% at 10 μM and sodium channel site 2, 83% at 10 μM);
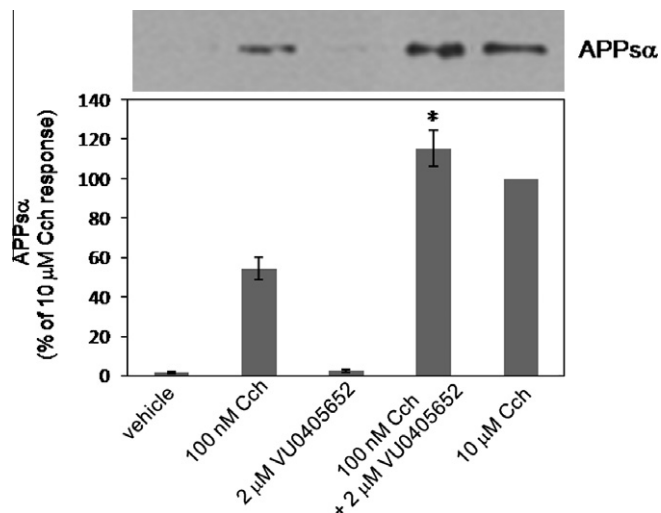

Figure 5. M_1 PAM VU04505652 (ML169) potentiates the CCh-mediated non-amyloidogenic APPsα release in TREx293-hM_1 cells.

importantly, **15j** was selective versus the biogenic amines (D_2, H-HT_2B, etc. . .) and displayed no orthosteric binding at M_1–M_5. Based on the exciting in vitro profile, we then evaluated **15j** for brain penetration in rat. A 10 mg/kg IP dose of **15j** afforded a brain$_{AUC}$/plasma$_{AUC}$ of 0.32 at 1 h, providing an improvement over both **3** (ML137) and BQCA with brain$_{AUC}$/plasma$_{AUC}$ of ~0.1. Based on this profile, **15j** (VU0405652) was declared an MLPCN probe, ML169.

As we have previously demonstrated with both an M_1 PAM (BQCA)[20] and M_1 allosteric agonists (**2**, ML071 and TBPB),[23] ML169 also shifted APP processing towards a non-amyloidogenic pathway.[24] As shown in Figure 5 10 μM carbachol (CCh) affords a significant increase in soluble APP (APPsα), while 100 nM CCh provides a modest increase. VU0405652 (ML169) at a dose of 2 μM has no effect, but in combination with low dose CCh (100 nM), ML169 potentiates the CCh-mediated non-amyloidogenic APPsα release to the same degree as 10 μM CCh. These data once again suggest that selective activation of M_1 may have a disease modifying role in Alzheimer's disease.[14,20]

In summary, we have developed a potent, selective and brain penetrant M_1 PAM, ML169, based on a novel indole scaffold from an MLPCN functional HTS. Further in vivo evaluation of this probe is underway and results from preclinical models of Alzheimer's disease and schizophrenia will be reported in due course. ML169 is an MLPCN probe and freely available upon request.

Acknowledgments

References and notes

1. Bonner, T. I.; Buckley, N. J.; Young, A. C.; Brann, M. R. Science **1987**, 237, 527.
2. Bonner, T. I.; Young, A. C.; Brann, M. R.; Buckley, N. J. Neuron **1988**, 1, 403.
3. Wess, J. Annu. Rev. Pharmacol. Toxicol. **2004**, 44, 423.
4. Langmead, C. J.; Watson, J.; Reavill, C. Pharmacol. Ther. **2008**, 117, 232.
5. Conn, P. J.; Jones, C.; Lindsley, C. W. Trends Pharmacol. Sci. **2009**, 30, 25.
6. Conn, P. J.; Lindsley, C. W.; Jones, C. Trends Pharmacol. Sci. **2009**, 30, 148.
7. Conn, P. J.; Christopoulos, A.; Lindsley, C. W. Nat. Rev. Durg Disc. **2009**, 8, 41.
8. Bridges, T. M.; LeBois, E. P.; Hopkins, C. R.; Wood, M. R.; Jones, J. K.; Conn, P. J.; Lindsley, C. W. Drug News Perspect. **2010**, 23, 229.
9. Lewis, J. A.; Lebois, E. P.; Lindsley, C. W. Curr. Opin. Chem. Biol. **2008**, 12, 269.
10. Digby, G. J.; Conn, P. J.; Lindsley, C. W. Curr. Opin. Drug Disc. Dev. **2010**, 13, 577.

11. Marlo, J. E.; Niswender, C. M.; Luo, Q.; Brady, A. E.; Shirey, J. K.; Rodriguez, A. L.; Bridges, T. M.; Williams, R.; Days, E.; Nalywajko, N. T.; Austin, C.; Williams, M.; Xiang, Y.; Orton, D.; Brown, H. A.; Kim, K.; Lindsley, C. W.; Weaver, C. D.; Conn, P. J. *Mol. Pharm.* **2009**, *75*(3), 577.
12. For information on the MLPCN and information on how to request probe compounds, such as ML169, see: http://mli.nih.gov/mli/mlpcn/.
13. Sheffler, D. J.; Williams, R.; Bridges, T. M.; Lewis, L. M.; Xiang, Z.; Zheng, F.; Kane, A. S.; Byum, N. E.; Jadhav, S.; Mock, M. M.; Zheng, F.; Lewis, L. M.; Jones, C. K.; Niswender, C. M.; Weaver, C. D.; Conn, P. J.; Lindsley, C. W.; Conn, P. J. *Mol. Pharmacol.* **2009**, *76*, 356.
14. Lebois, E. P.; Bridges, T. M.; Dawson, E. S.; Kennedy, J. p.; Xiang, Z.; Jadhav, S. B.; Yin, H.; Meiler, J.; Jones, C. K.; Conn, P. J. .; Weaver, C. D.; Lindsley, C. W. *ACS Chem. Neurosci.* **2010**, *1*, 104.
15. Bridges, T. M.; Kennedy, J. P.; Cho, H. P.; Conn, P. J.; Lindsley, C. W. *Bioorg. Med. Chem. Lett.* **2010**, *20*, 1972.
16. Bridges, T. M.; Marlo, J. E.; Niswender, C. M.; Jones, J. K.; Jadhav, S. B.; Gentry, P. R.; Weaver, C. D.; Conn, P. J.; Lindsley, C. W. *J. Med. Chem.* **2009**, *52*, 3445.
17. Bridges, T. M.; Kennedy, J. P.; Cho, H. P.; Conn, P. J.; Lindsley, C. W. *Bioorg. Med. Chem. Lett.* **2010**, *20*, 558.
18. Bridges, T. M.; Kennedy, J. P.; Hopkins, C. R.; Conn, P. J.; Lindsley, C. W. *Bioorg. Med. Chem. Lett.* **2010**, *20*, 5617.
19. Ma, L.; Seager, M.; Wittman, M.; Bickel, N.; Burno, M.; Jones, K.; Graufelds, V. K.; Xu, G.; Pearson, M.; McCampbell, A.; Gaspar, R.; Shughrue, P.; Danzinger, A.; Regan, C.; Garson, S.; Doran, S.; Kreatsoulas, C.; Veng, L.; Lindsley, C. W.; Shipe, W.; Kuduk, S.; Jacobson, M.; Sur, C.; Kinney, G.; Seabrook, G. R.; Ray, W. J. *Proc. Natl. Acad Sci. U.S.A.* **2009**, *106*, 15950.
20. Shirey, J. K.; Brady, A. E.; Jones, P. J.; Davis, A. A.; Bridges, T. M.; Jadhav, S. B.; Menon, U.; Christain, E. P.; Doherty, J. J.; Quirk, M. C.; Snyder, D. H.; Levey, A. I.; Watson, M. L.; Nicolle, M. M.; Lindsley, C. W.; Conn, P. J. *J. Neurosci.* **2009**, *29*, 14271.
21. Yang, F. V.; Shipe, W. D.; Bunda, J. L.; Nolt, M. B.; Wisnoski, D. D.; Zhao, Z.; Barrow, J. C.; Ray, W. J.; Ma, L.; Wittman, M.; Seager, M.; Koeplinger, K.; Hartman, G. D.; Lindsley, C. W. *Bioorg. Med. Chem. Lett.* **2010**, *20*, 531.
22. **ML169, 2-((1-(5-bromo-2-fluorobenzyl)-1***H***-indol-3-yl)sulfonyl)-***N***-(5-methylisoxazol-3-yl)acetamide.** To a solution of indole (3.00 g, 25.6 mmol) and methyl thioglycolate **8** (2.40 mL, 25.6 mmol) in methanol:water (80 mL: 20 mL) was added iodine (6.50 g, 25.6 mmol) and potassium iodide (4.25 g, 25.6 mmol). The reaction mixture was stirred at ambient temperature for 60 h. Methanol was removed *in vacuo* and the aqueous layer diluted with a saturated solution of sodium bicarbonate and extracted with ethyl acetate. The organic layer was dried over magnesium sulfate, evaporated *in vacuo* and the resulting residue was purified on a silica gel column (0–100% ethyl acetate:hexanes over 33 min) to afford the ester as an oil (LCMS >98%). The ester was dissolved in a mixture of tetrahydrofuran (20 mL) and 2.0 M aqueous LiOH (15 mL), then stirred vigorously at ambient temperature for 30 min. Tetrahydrofuran was removed *in vacuo*, the aqueous layer neutralized with 1.2 N HCl and extracted with CH_2Cl_2. The organic layer was dried over magnesium sulfate and removed *in vacuo* to produce an oily residue. Upon diluting the residue in dichloromethane a reddish-brown solid formed which was filtered and dried to yield compound **9** (2.00 g, 9.65 mmol, 38% yield over two steps, LCMS >98%). Compound **10** (650 mg, 3.14 mmol), 3-amino-5-methyl-isoxazole (616 mg, 6.28 mmol), PyClU (2.00 g, 6.28 mmol), and DIEA (1.36 mL, 7.85 mmol) were added to dichloroethane (25 mL) and microwave irradiated at 110 °C for 20 min. After cooling, the solvent was removed *in vacuo* and the remaining residue purified on a silica gel column (0–70% ethyl acetate:hexanes over 33 min) to yield compound **11** (642 mg, 2.23 mmol, 71% yield, LCMS >98%). Compound **11** (502 mg, 1.77 mmol) was dissolved in 25 mL (9:1, methanol:water) and Oxone (10.0 g, 17.7 mmol) was added. Stirring at ambient temperature continued overnight. Water (20 mL) was added and the mixture extracted with ethyl acetate (3 × 20 mL). The organics were combined, dried over magnesium sulfate, and concentrated *in vacuo* to give an oily residue which was purified on silica gel (0–50% ethyl acetate:hexanes over 19 min) to yield compound **12** (500 mg, 1.57 mmol, 88% yield, LCMS >98%). In a 5 mL microwave vial, compound **12** (55.0 mg, 0.174 mmol) was dissolved in DMF (3 mL) and cooled to 0 °C. Sodium hydride (60% by weight, 14.0 mg, 0.348 mmol) was then added in one portion and the reaction mixture vigorously stirred at 0 °C for 15 min. 4-Bromo-2-bromomethyl-1-flouro-benzene (51.0 mg, 0.191 mmol) was added in one portion and the reaction mixture was stirred while being allowed to warm to ambient temperature over 3 h. The reaction mixture was quenched with water (2 mL) and the solution was extracted with ethyl acetate (3 × 4 mL). The combined organics were dried over magnesium sulfate, concentrated *in vacuo* to give an oily residue which was purified on silica gel (0–70% ethyl acetate:hexanes over 19 min) to yield **ML169** (45 mg, 0.088 mmol, 51% yield). LCMS >98% 214 nm, t_R = 1.34 min, m/z = 506 ([^{79}Br]m+1), 508 ([^{81}Br]m+1). ^{1}H NMR (400 MHz, DMSO-d_6) 11.27 (s, 1H), 8.23 (s, 1H), 7.82 (d, J = 8.0 Hz, 1H), 7.63 (d, J = 8.0 Hz, 1H), 7.56–7.58 (m, 1H), 7.47 (dd, J = 2.4 Hz, 6.4 Hz, 1H), 7.35–7.23 (m, 3H), 6.54 (s, 1H), 5.62 (s, 2H), 4.43 (s, 2H), 2.37 (s, 3H), HRMS found: 506.0184; calculated for $C_{21}H_{17}BrFN_3O_4S$: 506.0.
23. Jones, C. K.; Brady, A. E.; Davis, A. A.; Xiang, Z.; Bubser, M.; Tantawy, M. N.; Kane, A.; Bridges, T. M.; Kennedy, J. P.; Bradley, S. R.; Peterson, T.; Baldwin, R. M.; Kessler, R.; Deutch, A.; Lah, J. L.; Levey, A. I.; Lindsley, C. W.; Conn, P. J. *J. Neurosci.* **2008**, *28*(41), 10422.
24. *APP processing.* In order to test the effect of M_1 PAM on M_1-stimulated APPsα release, a human M1 overexpressing stable cell line was generated in TREx293 cells (Invitrogen). Cells were plated at 0.3×10^6 cells in 6-well plate 2 days prior to experiments. Cells were pretreated with 2 μM VU0405652 or dimethylsulfoxide (DMSO) for 15 min. Immediately, 100 nM or 10 μM carbachol was added, and the medium was then conditioned for 1 h at 37 °C. Western blot analysis of the endogenous APPsα in conditioned media was performed as described.[23]